Electronic Supplementary Material (ESI) for Dalton Transactions
This journal is © The Royal Society of Chemistry 2013

Synthesis, Characterization and Structural Investigation of Novel *meso*-Pyridyl BODIPY–Cobaloxime Complexes

Juergen Bartelmess,[a] *Walter W. Weare,**[a] *Roger D. Sommer*[a]

[a] Department of Chemistry, North Carolina State University, Campus Box 8204, Raleigh, NC, 27695-8204, United States of America

wwweare@ncsu.edu

Crystallography

Page

S3-S6 Numbered molecular structures and crystallographic procedures for complexes **1**-**4**.

S7 Full sample and crystal data. Details about data collection and crystal refinement for BODIPY - cobaloxime complexes **1**-**4**.

S8 Selected bond lengths [Å] and angles [deg] for BODIPY-cobaloxime complexes **1**-**4**.

Electrochemistry

Page

S9-S13 Square wave and Cyclic voltammograms of complex **1**-**5** in dichloromethane and acetonitrile.

Spectroscopy

Page

S14-S17 Absorption and fluorescence spectra of BODIPY-cobaloxime complexes **1**-**4** and BODIPY derivatives **1a**-**4a** in dichloromethane and acetonitrile.

S18-S19 Solid state ATR-FT-IR spectra of compounds **1**-**4**.

S20-S23 ^{1}H and ^{13}C NMR spectra of complexes **1**-**4**.

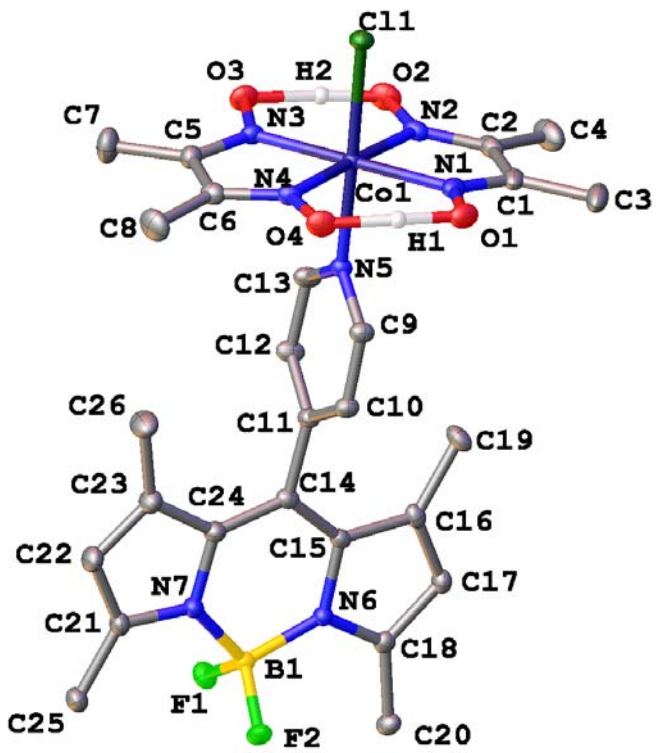

Figure S1. Numbered molecular structure of BODIPY-cobaloxime complex **1**. Thermal ellipsoids displaying 50% probability level. Hydrogen atoms (except bridging hydrogen atoms of the cobaloxime macrocycle) are omitted for clarity.

An orange plate-like specimen of $C_{26}H_{32}BClCoF_2N_7O_4$, approximate dimensions 0.050 mm x 0.200 mm x 0.400 mm, was used for the X-ray crystallographic analysis. A total of 856 frames were collected. The total exposure time was 2.38 hours. The frames were integrated with the Bruker SAINT software package using a narrow-frame algorithm. The integration of the data using a monoclinic unit cell yielded a total of 32625 reflections to a maximum θ angle of 31.51° (0.68 Å resolution), of which 9829 were independent (average redundancy 3.319, completeness = 99.9%, R_{int} = 3.04%, R_{sig} = 3.52%) and 7724 (78.58%) were greater than $2\sigma(F^2)$. The final cell constants of a = 14.3775(6) Å, b = 14.6934(5) Å, c = 14.0989(6) Å, β = 97.256(2)°, volume = 2954.6(2) $Å^3$, are based upon the refinement of the XYZ-centroids of 9989 reflections above 20 σ(I) with 5.140° < 2θ < 66.77°. Data were corrected for absorption effects using the multi-scan method (SADABS). The ratio of minimum to maximum apparent transmission was 0.900.

The structure was solved and refined using the Bruker SHELXTL Software Package, using the space group $P2_1/c$, with Z = 4 for the formula unit, $C_{26}H_{32}BClCoF_2N_7O_4$. The final anisotropic full-matrix least-squares refinement on F^2 with 393 variables converged at R1 = 3.37%, for the observed data and wR2 = 8.61% for all data. The goodness-of-fit was 1.022. The largest peak in the final difference electron density synthesis was 0.436 $e^-/Å^3$ and the largest hole was -0.394 $e^-/Å^3$ with an RMS deviation of 0.066 $e^-/Å^3$. On the basis of the final model, the calculated density was 1.461 g/cm^3 and F(000), 1344 e^-.

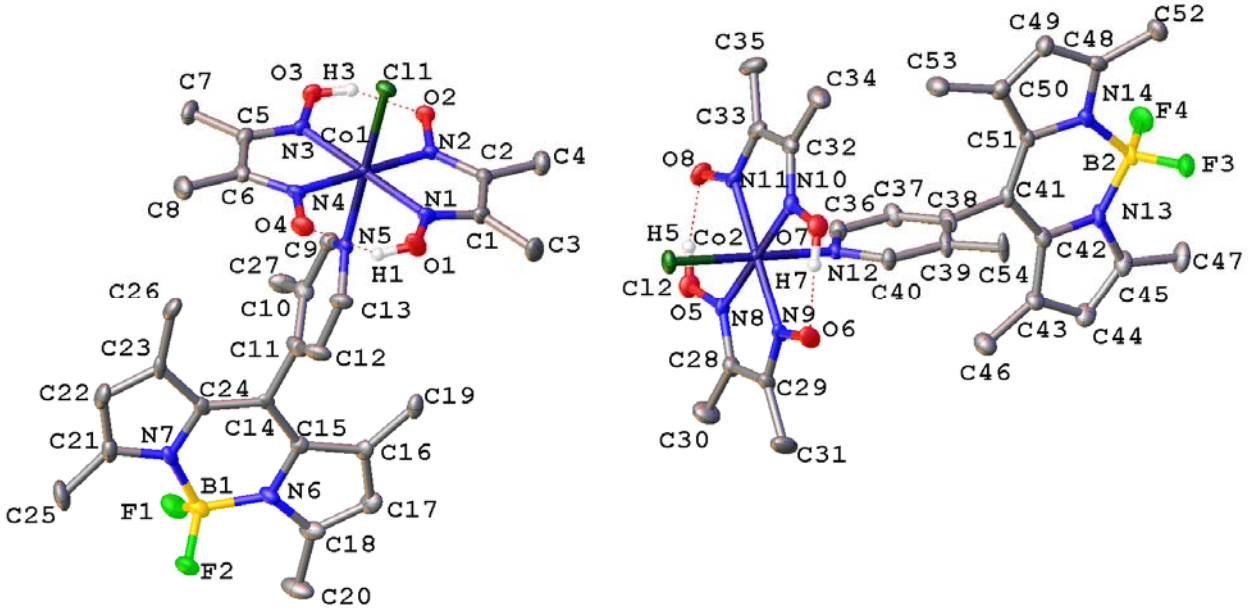

Figure S2. Numbered molecular structure of BODIPY-cobaloxime complex **2** (**2A** left and **2B** right). The two independent molecular structures of the highest probability, found in one single crystal, are shown. Thermal ellipsoids displaying 50% probability level. Hydrogen atoms (except bridging hydrogen atoms of the cobaloxime macrocycle) are omitted for clarity.

A dark red-orange block-like specimen of $C_{27}H_{34}BClCoF_2N_7O_4$, approximate dimensions 0.210 mm x 0.270 mm x 0.340 mm, was used for the X-ray crystallographic analysis. The X-ray intensity data were measured. A total of 1439 frames were collected. The total exposure time was 11.99 hours. The frames were integrated with the Bruker SAINT software package using a narrow-frame algorithm. The integration of the data using a monoclinic unit cell yielded a total of 108930 reflections to a maximum θ angle of 30.51° (0.70 Å resolution), of which 18312 were independent (average redundancy 5.949, completeness = 100.9%, R_{int} = 3.69%, R_{sig} = 2.72%) and 16245 (88.71%) were greater than $2\sigma(F^2)$. The final cell constants of a = 16.6111(5) Å, b = 13.0356(4) Å, c = 27.7368(10) Å, β = 90.834(2)°, volume = 6005.4(3) $Å^3$, are based upon the refinement of the XYZ-centroids of 9565 reflections above 20 σ(I) with 4.904° < 2θ < 66.16°. Data were corrected for absorption effects using the multi-scan method (SADABS). The ratio of minimum to maximum apparent transmission was 0.884. The calculated minimum and maximum transmission coefficients (based on crystal size) are 0.7920 and 0.8640.

The structure was solved and refined using the Bruker SHELXTL Software Package, using the space group $P2_1/c$, with Z = 8 for the formula unit, $C_{27}H_{34}BClCoF_2N_7O_4$. The final anisotropic full-matrix least-squares refinement on F^2 with 1144 variables converged at R1 = 5.74%, for the observed data and wR2 = 12.52% for all data. The goodness-of-fit was 1.227. The largest peak in the final difference electron density synthesis was 0.883 $e^-/Å^3$ and the largest hole was -0.787 $e^-/Å^3$ with an RMS deviation of 0.085 $e^-/Å^3$. On the basis of the final model, the calculated density was 1.468 g/cm^3 and F(000), 2752 e^-.

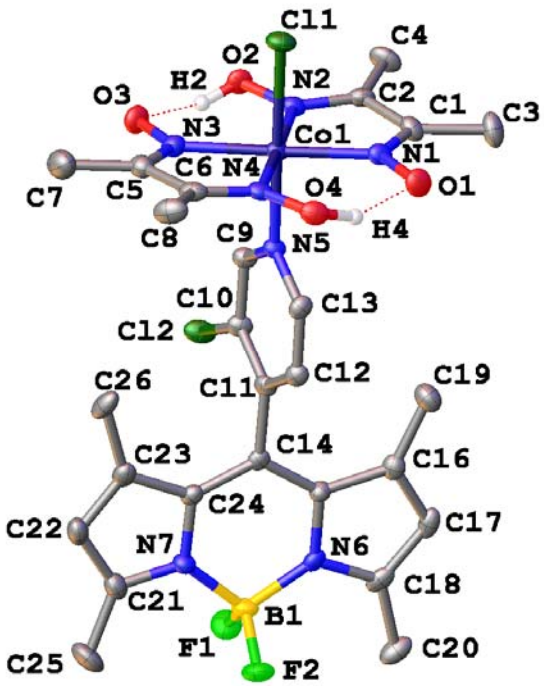

Figure S3. Numbered molecular structure of BODIPY-cobaloxime complex **3**. Thermal ellipsoids displaying 50% probability level. Hydrogen atoms (except bridging hydrogen atoms of the cobaloxime macrocycle) and solvent molecules (one molecule of dichloromethane) are omitted for clarity.

A clear orange-red needle-like specimen of $C_{27}H_{33}BCl_4CoF_2N_7O_4$, approximate dimensions 0.100 mm x 0.100 mm x 0.400 mm, was used for the X-ray crystallographic analysis. The X-ray intensity data were measured on a Bruker-Nonius X8 Kappa APEX II system equipped with a graphite monochromator and a MoKα fine-focus sealed tube (λ = 0.71073 Å). A total of 1119 frames were collected. The total exposure time was 6.22 hours. The frames were integrated with the Bruker SAINT software package using a narrow-frame algorithm. The integration of the data using an orthorhombic unit cell yielded a total of 44132 reflections to a maximum θ angle of 28.50° (0.74 Å resolution), of which 8754 were independent (average redundancy 5.041, completeness = 99.9%, R_{int} = 4.80%, R_{sig} = 4.86%) and 7457 (85.18%) were greater than $2\sigma(F^2)$. The final cell constants of a = 9.8118(3) Å, b = 15.3669(4) Å, c = 22.9114(5) Å, volume = 3454.51(16) $Å^3$, are based upon the refinement of the XYZ-centroids of 9959 reflections above 20 σ(I) with 4.515° < 2θ < 51.91°. Data were corrected for absorption effects using the multi-scan method (SADABS). The ratio of minimum to maximum apparent transmission was 0.914. The calculated minimum and maximum transmission coefficients (based on crystal size) are 0.7250 and 0.9190.

The structure was solved and refined using the Bruker SHELXTL Software Package, using the space group $P2_12_12_1$, with Z = 4 for the formula unit, $C_{27}H_{33}BCl_4CoF_2N_7O_4$. The final anisotropic full-matrix least-squares refinement on F^2 with 430 variables converged at R1 = 5.80%, for the observed data and wR2 = 17.32% for all data. The goodness-of-fit was 1.042. The largest peak in the final difference electron density synthesis was 1.459 $e^-/Å^3$ and the largest hole was -1.193 $e^-/Å^3$ with an RMS deviation of 0.133 $e^-/Å^3$. On the basis of the final model, the calculated density was 1.479 g/cm^3 and F(000), 1576 e^-.

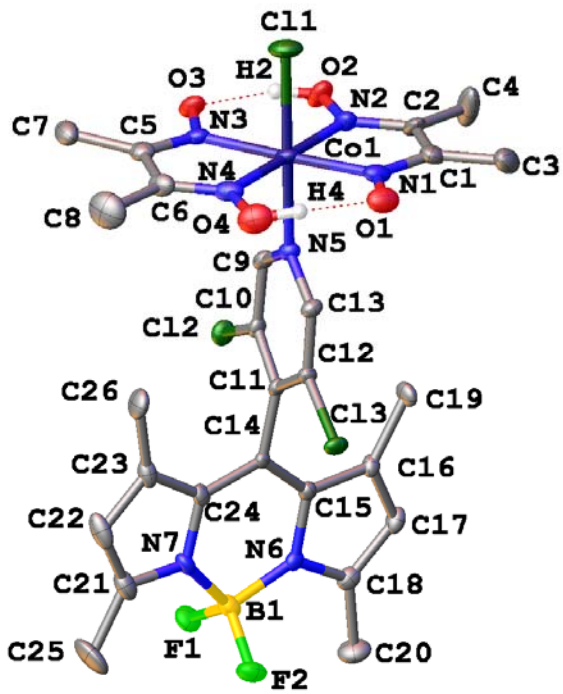

Figure S4. Numbered molecular structure of BODIPY-cobaloxime complex **4**. Thermal ellipsoids displaying 50% probability level. Hydrogen atoms (except bridging hydrogen atoms of the cobaloxime macrocycle) and solvent molecules (one molecule of dichloromethane) are omitted for clarity.

A dark red needle-like specimen of $C_{27}H_{32}BCl_5CoF_2N_7O_4$, approximate dimensions 0.100 mm x 0.500 mm x 0.500 mm, was used for the X-ray crystallographic analysis. The X-ray intensity data were measured. A total of 1028 frames were collected. The total exposure time was 2.86 hours. The frames were integrated with the Bruker SAINT software package using a narrow-frame algorithm. The integration of the data using an orthorhombic unit cell yielded a total of 52258 reflections to a maximum θ angle of 33.16° (0.65 Å resolution), of which 13569 were independent (average redundancy 3.851, completeness = 99.7%, R_{int} = 4.67%, R_{sig} = 3.24%) and 11017 (81.19%) were greater than $2\sigma(F^2)$. The final cell constants of a = 10.6796(4) Å, b = 15.1701(6) Å, c = 22.0725(8) Å, volume = 3576.0(2) $Å^3$, are based upon the refinement of the XYZ-centroids of 9886 reflections above 20 σ(I) with 4.564° < 2θ < 57.88°. Data were corrected for absorption effects using the multi-scan method (SADABS). The ratio of minimum to maximum apparent transmission was 0.795. The calculated minimum and maximum transmission coefficients (based on crystal size) are 0.6600 and 0.9150.

The structure was solved and refined using the Bruker SHELXTL Software Package, using the space group $P2_12_12_1$, with Z = 4 for the formula unit, $C_{27}H_{32}BCl_5CoF_2N_7O_4$. The final anisotropic full-matrix least-squares refinement on F^2 with 439 variables converged at R1 = 8.38%, for the observed data and wR2 = 23.32% for all data. The goodness-of-fit was 1.057. The largest peak in the final difference electron density synthesis was 3.313 $e^-/Å^3$ and the largest hole was -2.309 $e^-/Å^3$ with an RMS deviation of 0.167 $e^-/Å^3$. On the basis of the final model, the calculated density was 1.493 g/cm^3 and F(000), 1640 e^-.

Table S1 Sample and crystal data, details about data collection and crystal refinement for BODIPY-cobaloxime complexes **1-4**.

Complex	**1**	**2**	**3**	**4**
Chemical formula	$C_{26}H_{32}BClCoF_2N_7O_4$	$C_{27}H_{34}BClCoF_2N_7O_4$	$C_{27}H_{33}BCl_4CoF_2N_7O_4$	$C_{27}H_{32}BCl_5CoF_2N_7O_4$
Formula weight	649.78	663.80	769.14	803.58
Temperature	110(2) K	110(2) K	100(2) K	100(2) K
Wavelength	0.71073 Å	0.71073 Å	0.71073 Å	0.71073 Å
Crystal size	0.050 x 0.200 x 0.400 mm	0.210 x 0.270 x 0.340 mm	0.100 x 0.100 x 0.400 mm	0.100 x 0.500 x 0.500 mm
Crystal habit	orange plate	dark red-orange block	clear orange-red needle	dark red needle
Crystal system	monoclinic	monoclinic	orthorhombic	orthorhombic
Space group	$P2_1/c$	$P2_1/c$	$P\ 2_1\ 2_1\ 2_1$	$P\ 2_1\ 2_1\ 2_1$
Unit cell dimensions	a = 14.3775(6) Å b = 14.6934(5) Å c = 14.0989(6) Å α = 90° β = 97.256(2)° γ = 90°	a = 16.6111(5) Å b = 13.0356(4) Å c = 27.7368(10) Å α = 90° β = 90.834(2)° γ = 90°	a = 9.8118(3) Å b = 15.3669(4) Å c = 22.9114(5) Å α = 90° β = 90° γ = 90°	a = 10.6796(4) Å b = 15.1701(6) Å c = 22.0725(8) Å α = 90° β = 90° γ = 90°
Volume	2954.6(2) $Å^3$	6005.4(3) $Å^3$	3454.51(16) $Å^3$	3576.0(2) $Å^3$
Z	4	8	4	4
Density (calculated)	1.461 g/cm^3	1.468 g/cm^3	1.479 g/cm^3	1.493 g/cm^3
Absorption coefficient	0.729 mm^{-1}	0.719 mm^{-1}	0.860 mm^{-1}	0.907 mm^{-1}
F(000)	1344	2752	1576	1640
Theta range for data collection	1.99 to 31.51°	1.23 to 30.51°	1.60 to 28.50°	1.63 to 33.16°
Index ranges	-21<=h<=21, -21<=k<=11, -20<=l<=20	-23<=h<=14, -18<=k<=18, -39<=l<=39	-13<=h<=13, -20<=k<=20, -30<=l<=30	-8<=h<=16, -23<=k<=23, -33<=l<=33
Reflections collected	32625	108930	44132	52258
Independent reflections	9829 [R(int) = 0.0304]	18312 [R(int) = 0.0369]	8754 [R(int) = 0.0480]	13569 [R(int) = 0.0467]
Coverage of independent reflections	99.9%	100.9%	99.9%	99.7%
Absorption correction	multi-scan	multi-scan	multi-scan	multi-scan
Max. and min. transmission	0.8640 and 0.7920	0.7920 and 0.8640	0.9190 and 0.7250	0.9150 and 0.6600
Structure solution technique	direct methods	direct methods	direct methods	direct methods
Structure solution program	SHELXS-97	SHELXS-97	SHELXS-97	SHELXS-97
Refinement method	Full-matrix least-squares on F^2	Full-matrix least-squares on F^2	Full-matrix least-squares on F^2	Full-matrix least-squares on F^2
Refinement program	SHELXL-97	SHELXL-2013	SHELXL-2013	SHELXL-2013
Function minimized	$\Sigma\ w(F_o^2 - F_c^2)^2$	$\Sigma\ w(F_o^2 - F_c^2)^2$	$\Sigma\ w(F_o^2 - F_c^2)^2$	$\Sigma\ w(F_o^2 - F_c^2)^2$
Data / restraints / parameters	9829 / 0 / 393	18312 / 823 / 1144	8754 / 0 / 430	13569 / 27 / 439
Goodness-of-fit on F^2	1.022	1.227	1.042	1.057
Final R indices	7724 data; I>2σ(I): R1 = 0.0337, wR2 = 0.0789 all data: R1 = 0.0508, wR2 = 0.0861	16245 data; I>2σ(I): R1 = 0.0574, wR2 = 0.1220 all data: R1 = 0.0654, wR2 = 0.1252	7457 data; I>2σ(I): R1 = 0.0580, wR2 = 0.1641 all data: R1 = 0.0727, wR2 = 0.1732	11017 data; I>2σ(I): R1 = 0.0838, wR2 = 0.2230 all data: R1 = 0.1002, wR2 = 0.2332
Weighting scheme	$w=1/[\sigma^2(F_o^2)+(0.0402P)^2+0.9787P]$ where $P=(F_o^2+2F_c^2)/3$	$w=1/[\sigma^2(F_o^2)+(0.0170P)^2+15.1833P]$ where $P=(F_o^2+2F_c^2)/3$	$w=1/[\sigma^2(F_o^2)+(0.1120P)^2+3.0925P]$ where $P=(F_o^2+2F_c^2)/3$	$w=1/[\sigma^2(F_o^2)+(0.1206P)^2+11.0643P]$ where $P=(F_o^2+2F_c^2)/3$
Largest diff. peak and hole	0.436 and -0.394 $eÅ^{-3}$	0.883 and -0.787 $eÅ^{-3}$	1.459 and -1.193 $eÅ^{-3}$	3.313 and -2.309 $eÅ^{-3}$
R.M.S. deviation from mean	0.066 $eÅ^{-3}$	0.085 $eÅ^{-3}$	0.133 $eÅ^{-3}$	0.167 $eÅ^{-3}$

Table S2. Selected bond lengths [Å] and angles [deg] for BODIPY-cobaloxime complexes **1**-**4**.

	1	**2A**[a]	**2B**[a]	**3**	**4**
N1-Co1	1.9038(12)	1.881(2)	1.888(2)	1.894(5)	1.898(6)
N2-Co1	1.9040(12)	1.876(2)	1.879(2)	1.907(5)	1.889(5)
N3-Co1	1.8852(11)	1.897(2)	1.898(3)	1.899(5)	1.902(6)
N4-Co1	1.8865(11)	1.903(2)	1.896(2)	1.892(5)	1.896(5)
Co1-Cl1	2.2293(4)	2.2234(8)	2.2117(2)	2.2300(14)	2.2184(17)
N1-N2	2.475	2.464	2.460	2.482	2.489
N3-N4	2.474	2.469	2.470	2.476	2.483
N1-N4	2.872	2.874	2.863	2.868	2.862
N2-N3	2.868	2.851	2.870	2.879	2.866
O1-O4	2.4779(16)	2.480	2.472	2.485(6)	2.473
O2-O3	2.4822(15)	2.477	2.483	2.467(7)	2.475
N5-Co1	1.9615(11)	1.961(2)	1.958(2)	1.966(4)	1.958(4)
C9-N5	1.3471(17)	1.342(4)	1.337(4)	1.340(7)	1.348(8)
C13-N5	1.3469(17)	1.351(4)	1.344(4)	1.354(7)	1.334(7)
C11-N5	2.787	2.772	2.770	2.794	2.807
C11-C14	1.4878(18)	1.485(5)	1.500(5)	1.489(7)	1.477(7)
Cl2-C10	n.a.	n.a.	n.a.	1.719(6)	1.714(6)
Cl3-C12	n.a.	n.a.	n.a.	n.a.	1.723(6)
C11-N5-Co1	173.7	170.0	169.1	178.0	174.1
Torsion C10-C11-C14-C15	92.9	89.7	90.9	102.3	82.4
Torsion C10-C11-C14-C24	87.1	88.8	79.8	77.5	96.2

[a] Complex **2** shows two independent crystal structure in one single crystal, structure are denoted **2A** and **2B**, respectively (structures of highest probability are shown). For the corresponding atom numbering of complex **2B**, see Figure S2.

n.a.: not applicable.

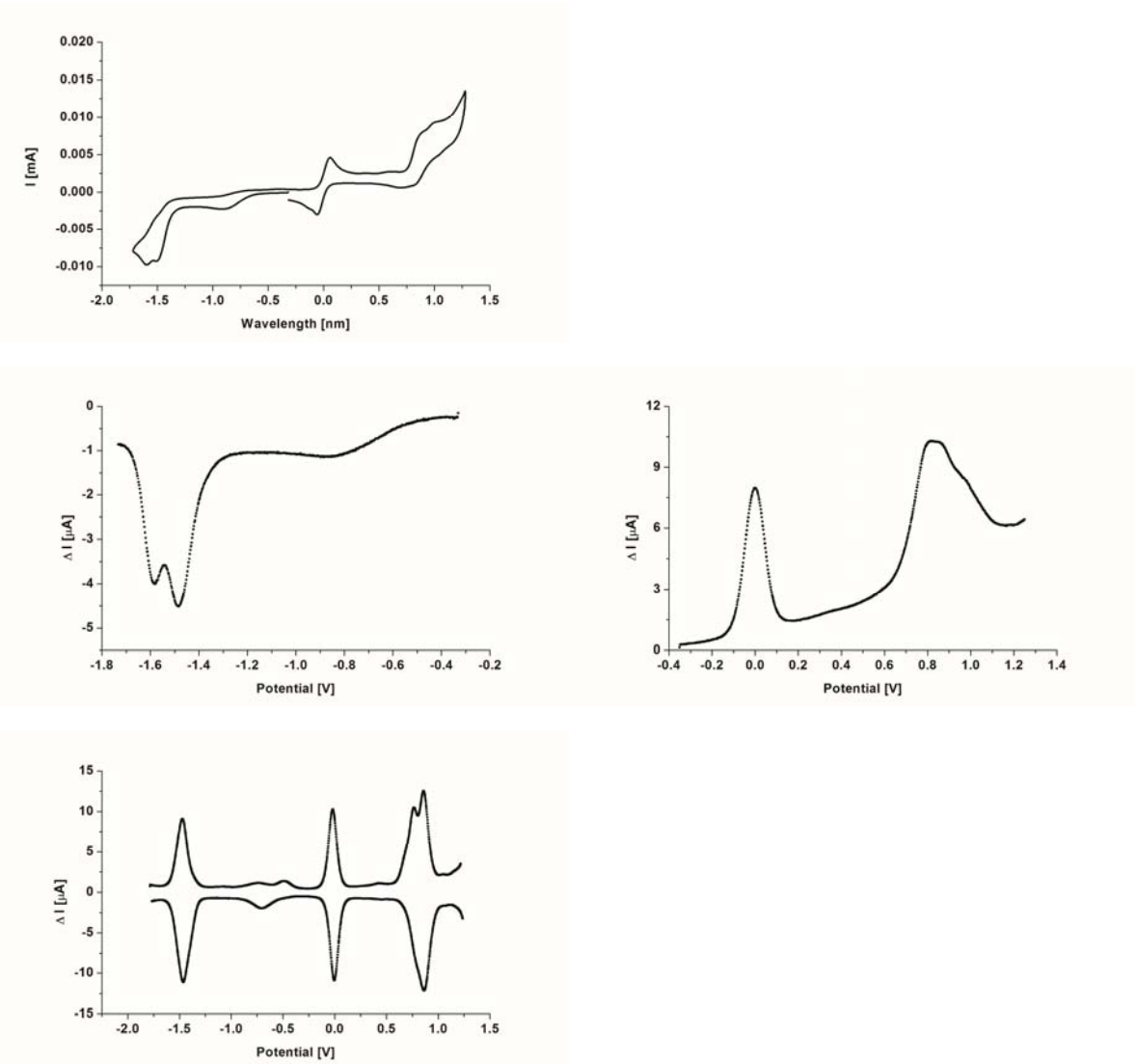

Figure S5.

TOP: Cyclic voltammogram (CV) of complex **1** in degassed dichloromethane.

CENTER: Complementary square wave voltammograms (SWV) illustrating the reduction (left) and oxidation (right) of complex **1** in degassed dichloromethane. SWV were recorded starting from 0 V (setting at the potentiostat) and later corrected for the reference wave $Fc/Fc^+ = 0$ V. Spectra recorded at 40 mV/s (for oxidation) or -40 mV/s (for reduction).

BOTTOM: SWV of complex **1** in degassed acetonitrile. Recorded sweeping from an initial reductive potential to the maximum oxidative potential and back to the initial negative potential. Corrected for the reference wave $Fc/Fc^+ = 0$ V. Measured at a scanrate of 40 mV/s.

All measurements with 0.1 M tetrabutylammonium hexafluorophosphate auxiliary electrolyte. Wave at 0 V represents the oxidation of ferrocene and is used as internal reference.

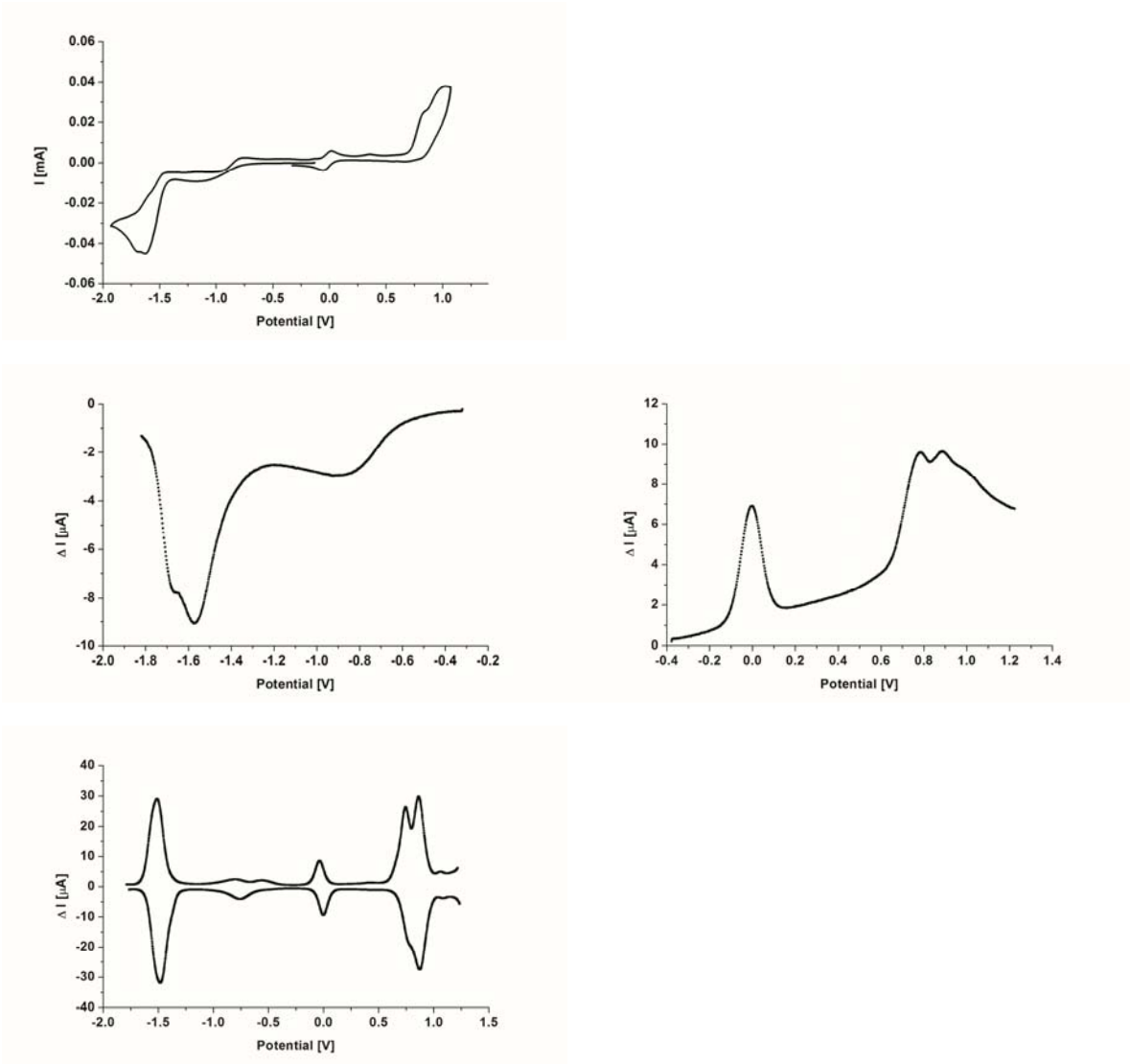

Figure S6.

TOP: Cyclic voltammogram (CV) of complex **2** in degassed dichloromethane (left) and acetonitrile (right).

CENTER: Complementary square wave voltammograms (SWV) illustrating the reduction (left) and oxidation (right) of complex **2** in degassed dichloromethane. SWV were recorded starting from 0 V (setting at the potentiostat) and later corrected for the reference wave $Fc/Fc^+ = 0$ V. Spectra recorded at 40 mV/s (for oxidation) or -40 mV/s (for reduction).

BOTTOM: SWV of complex **2** in degassed acetonitrile. Recorded sweeping from an initial reductive potential to the maximum oxidative potential and back to the initial negative potential. Corrected for the reference wave $Fc/Fc^+ = 0$ V. Measured at a scanrate of 40 mV/s.

All measurements with 0.1 M tetrabutylammonium hexafluorophosphate auxiliary electrolyte. Wave at 0 V represents the oxidation of ferrocene and is used as internal reference.

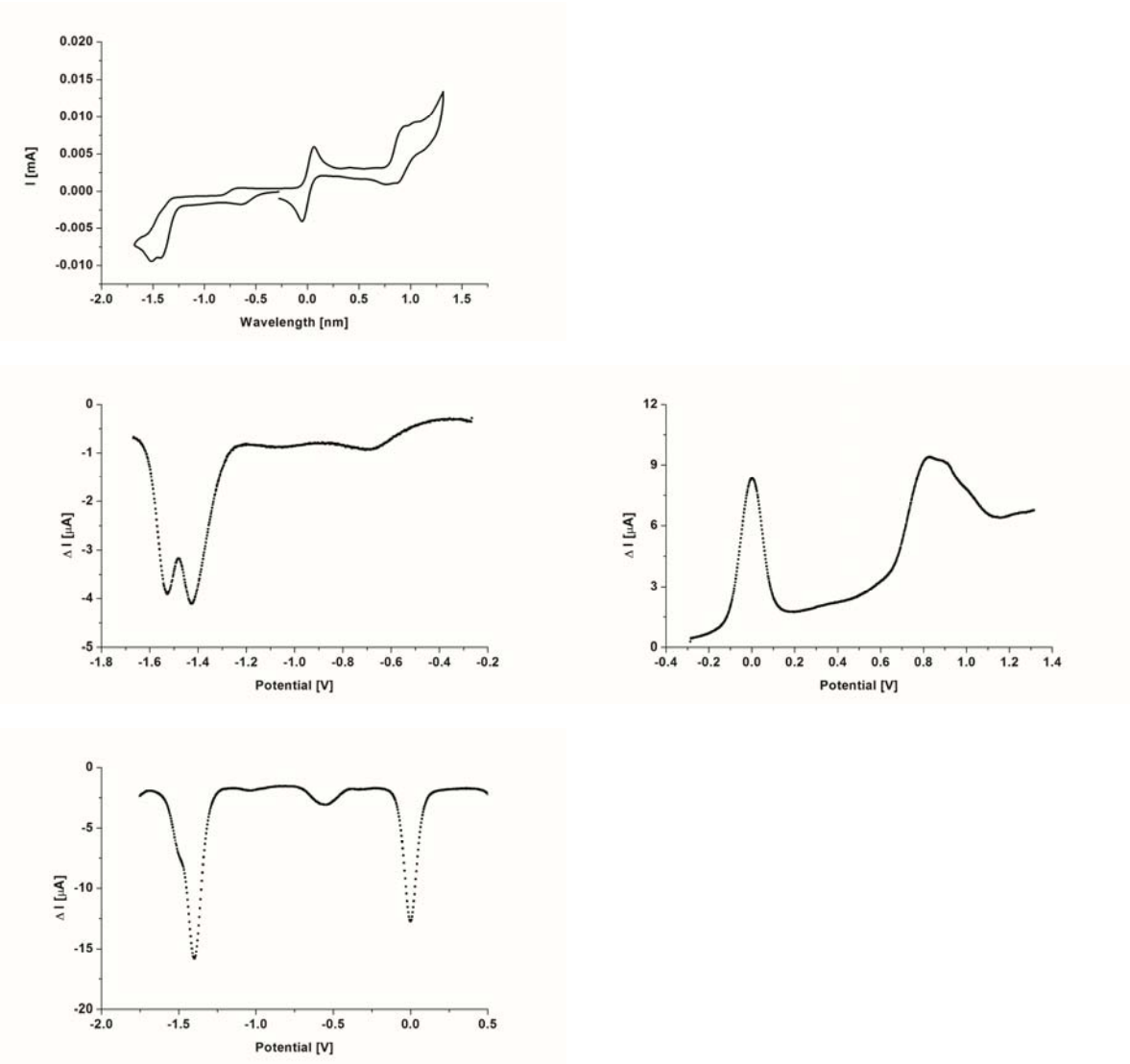

Figure S7.

TOP: Cyclic voltammogram (CV) of complex **3** in degassed dichloromethane (left) and acetonitrile (right).

CENTER: Complementary square wave voltammograms (SWV) illustrating the reduction (left) and oxidation (right) of complex **3** in degassed dichloromethane. SWV were recorded starting from 0 V (setting at the potentiostat) and later corrected for the reference wave Fc/Fc^+ = 0 V. Spectra recorded at 40 mV/s (for oxidation) or -40 mV/s (for reduction).

BOTTOM: SWV illustrating the reduction of complex **3** in degassed acetonitrile. Recorded sweeping from 0 V (setting at the potentiostat) to the initial minimum negative potential (-1.4 V on the potentiostat). Oxidative conditions lead to decomposition of the complex. Corrected for the reference wave Fc/Fc^+ = 0 V. Measured at a scanrate of 40 mV/s.

All measurements with 0.1 M tetrabutylammonium hexafluorophosphate auxiliary electrolyte. Wave at 0 V represents the oxidation of ferrocene and is used as internal reference.

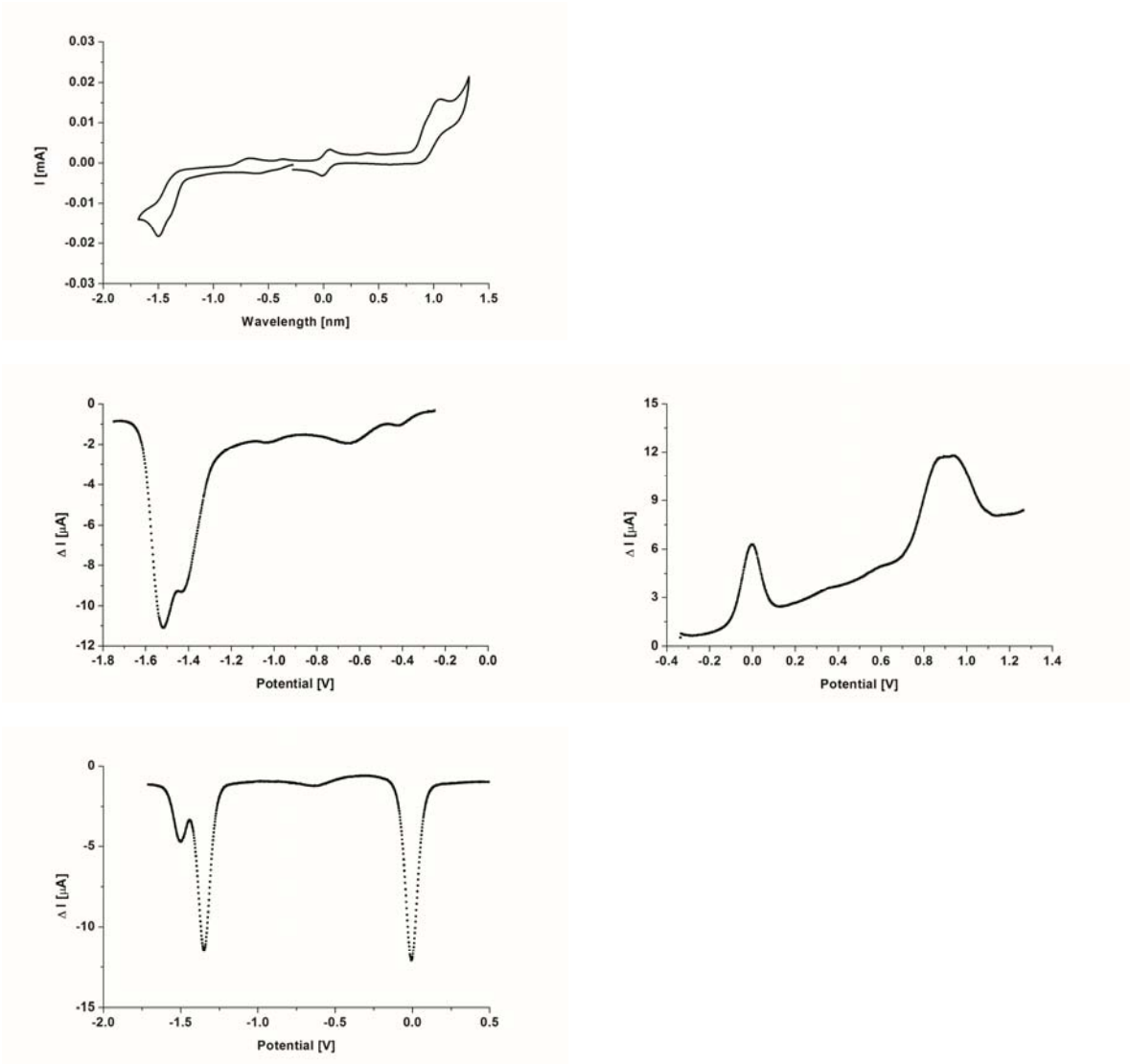

Figure S8.

TOP: Cyclic voltammogram (CV) of complex **4** in degassed dichloromethane (left) and acetonitrile (right).

CENTER: Complementary square wave voltammograms (SWV) illustrating the reduction (left) and oxidation (right) of complex **4** in degassed dichloromethane. SWV were recorded starting from 0 V (setting at the potentiostat) and later corrected for the reference wave Fc/Fc^+ = 0 V. Spectra recorded at 40 mV/s (for oxidation) or -40 mV/s (for reduction).

BOTTOM: SWV illustrating the reduction of complex **4** in degassed acetonitrile. Recorded sweeping from 0 V (setting at the potentiostat) to the initial minimum negative potential (-1.4 V on the potentiostat). Oxidative conditions lead to decomposition of the complex. Corrected for the reference wave Fc/Fc^+ = 0 V. Measured at a scanrate of 40 mV/s.

All measurements with 0.1 M tetrabutylammonium hexafluorophosphate auxiliary electrolyte. Wave at 0 V represents the oxidation of ferrocene and is used as internal reference.

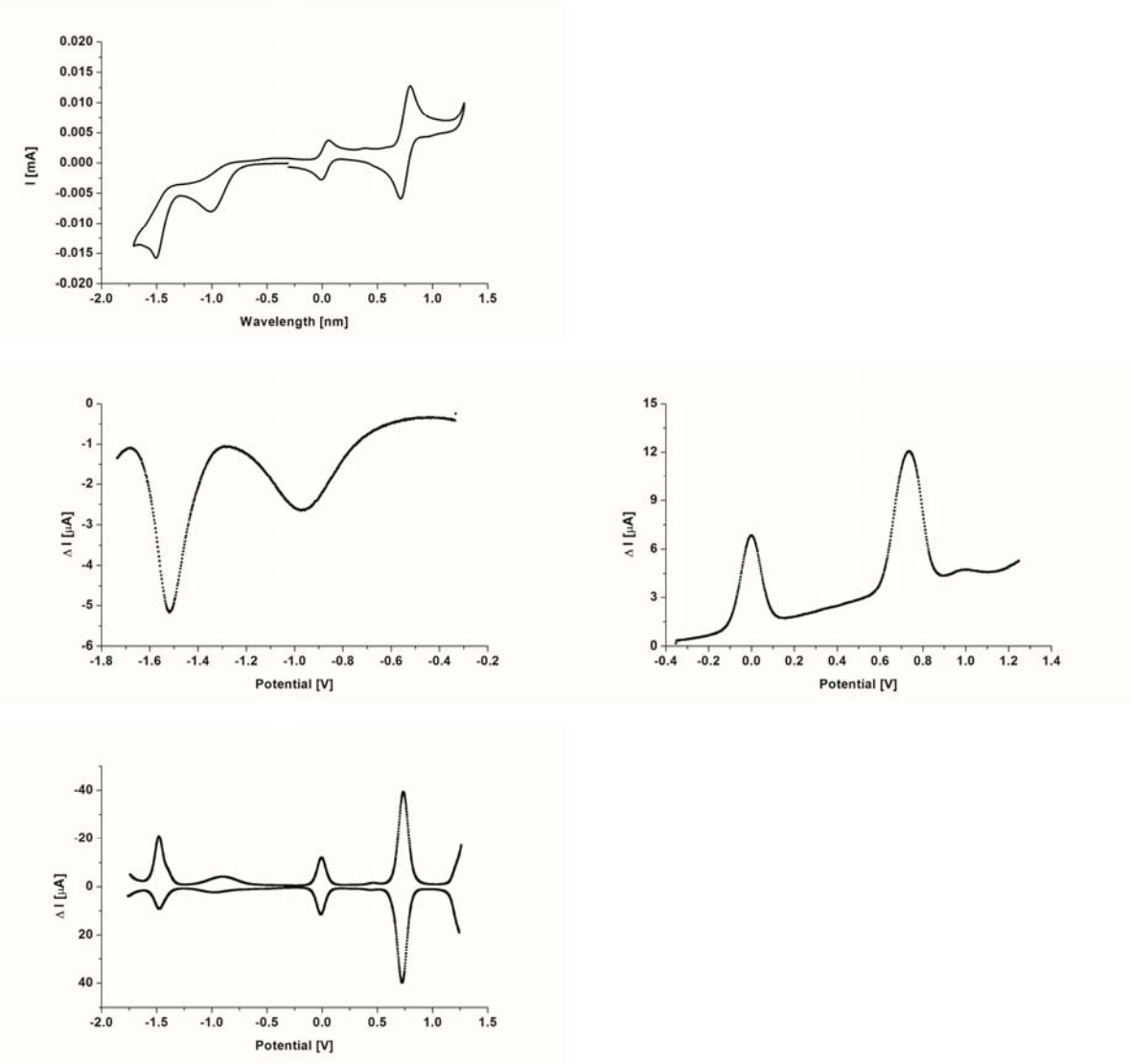

Figure S9.

TOP: Cyclic voltammogram (CV) of reference pyridyl-complex **5** (without photosensitizer and pending BODIPY) in degassed dichloromethane (left) and acetonitrile (right).

BOTTOM: Complementary square wave voltammograms (SWV) illustrating the reduction (left) and oxidation (right) of complex **5** in degassed dichloromethane. SWV were recorded starting from 0 V (setting at the potentiostat) and later corrected for the reference wave Fc/Fc^+ = 0 V. Spectra recorded at 40 mV/s (for oxidation) or -40 mV/s (for reduction).

BOTTOM: SWV of reference pyridyl-complex **5** in degassed acetonitrile. Recorded sweeping from an initial reductive potential to the maximum oxidative potential and back to the initial negative potential. Corrected for the reference wave Fc/Fc^+ = 0 V. Measured at a scanrate of 40 mV/s.

All measurements with 0.1 M tetrabutylammonium hexafluorophosphate auxiliary electrolyte. Wave at 0 V represents the oxidation of ferrocene and is used as internal reference.

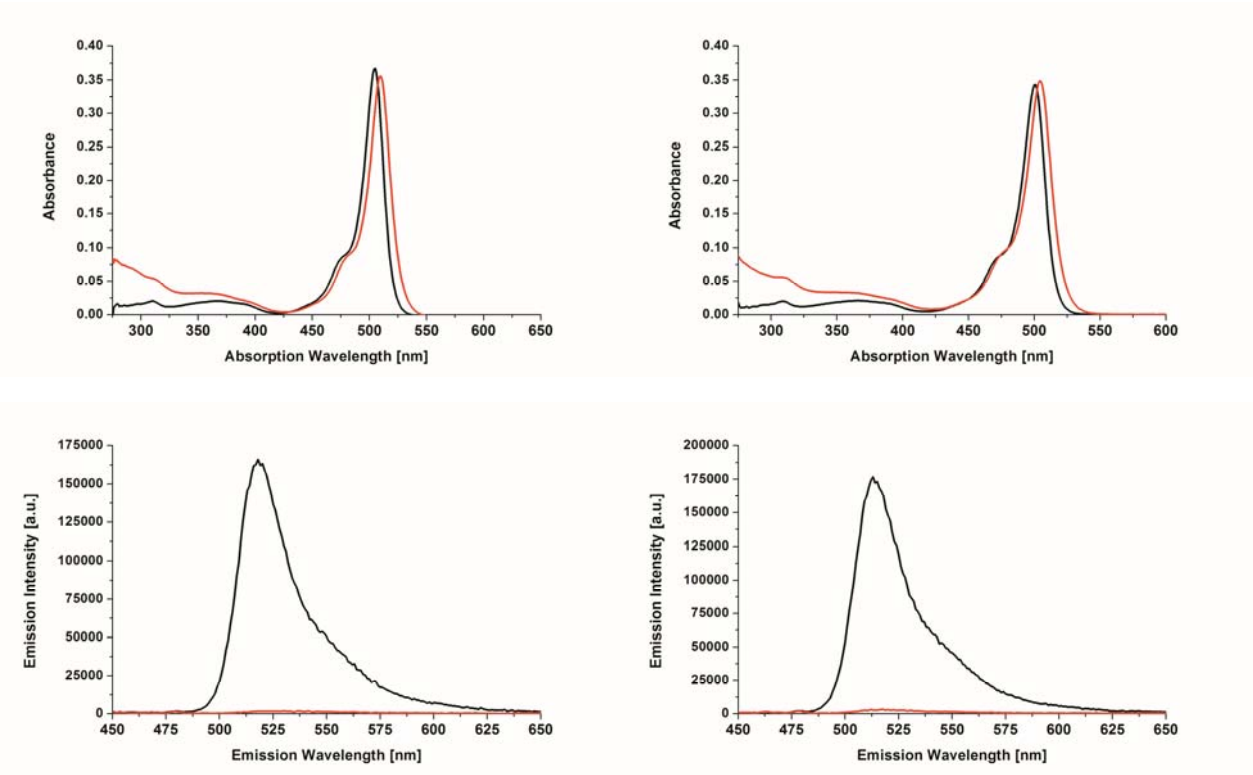

Figure S10. Absorption (top) and fluorescence (bottom) spectra of BODIPY **1a** (black line) and cobaloxime-BODIPY complex **1** (red line). Spectra acquired in dichloromethane (left column) and acetonitrile (right column) illustrating the fluorescence quenching of the BODIPY centered fluorescence upon complexation. Excitation wavelength at 420 nm. c = ~5 x 10^{-6} M.

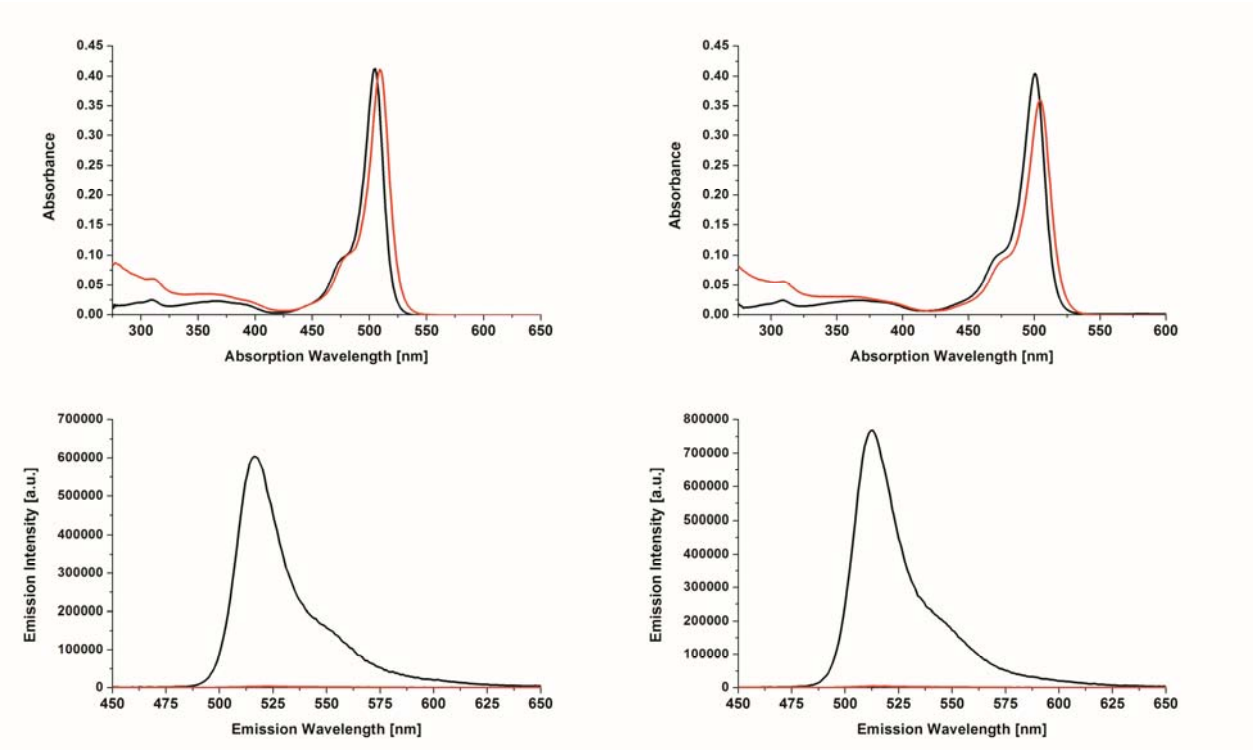

Figure S11. Absorption (top) and fluorescence (bottom) spectra of BODIPY **2a** (black line) and cobaloxime-BODIPY complex **2** (red line). Spectra acquired in dichloromethane (left column) and acetonitrile (right column) illustrating the fluorescence quenching of the BODIPY centered fluorescence upon complexation. Excitation wavelength at 420 nm. c = ~5 x 10^{-6} M.

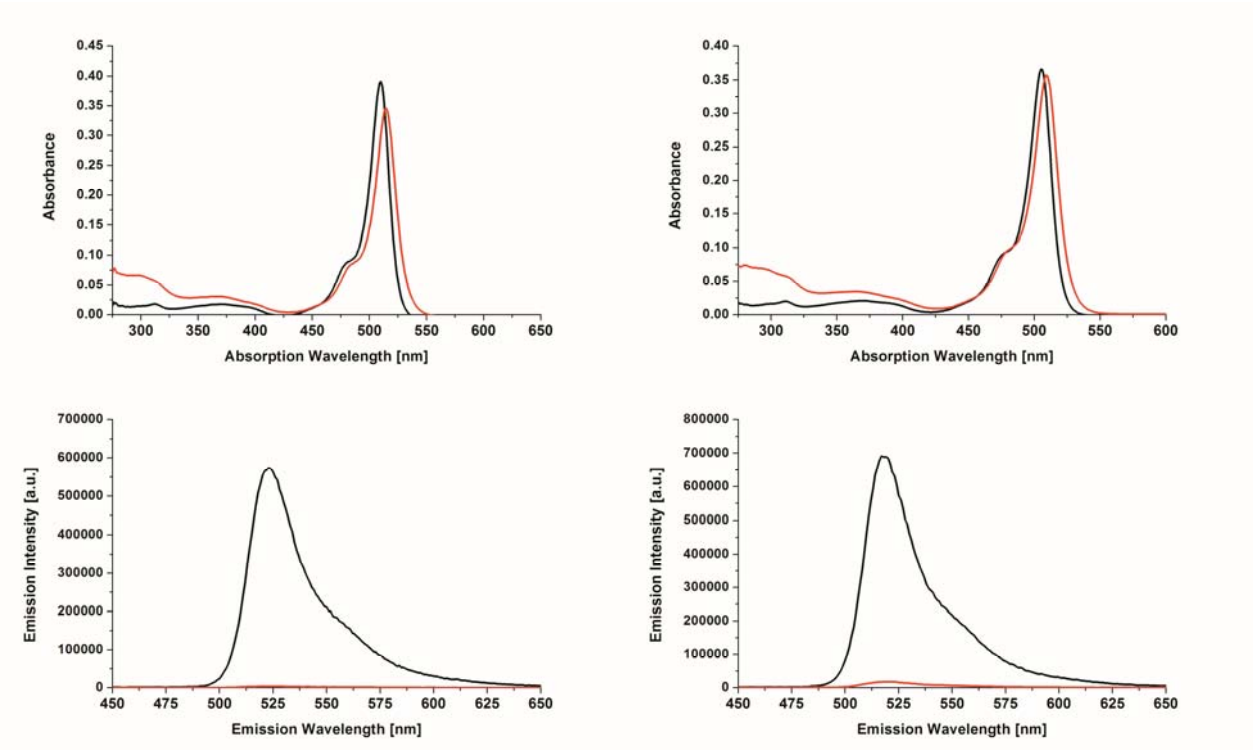

Figure S12. Absorption (top) and fluorescence (bottom) spectra of BODIPY **3a** (black line) and cobaloxime-BODIPY complex **3** (red line). Spectra acquired in dichloromethane (left column) and acetonitrile (right column) illustrating the fluorescence quenching of the BODIPY centered fluorescence upon complexation. Excitation wavelength at 425 nm. c = ~5 x 10^{-6} M.

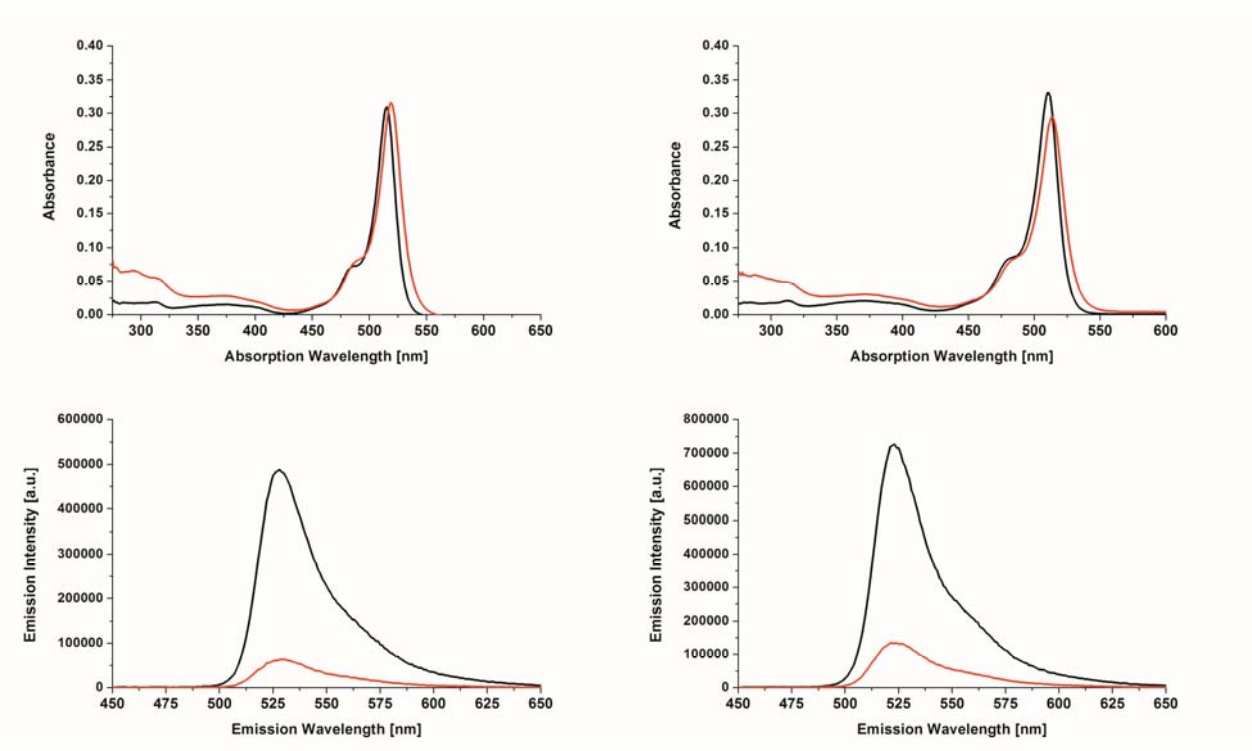

Figure S13. Absorption (top) and fluorescence (bottom) spectra of BODIPY **4a** (black line) and cobaloxime-BODIPY complex **4** (red line). Spectra acquired in dichloromethane (left column) and acetonitrile (right column) illustrating the fluorescence quenching of the BODIPY centered fluorescence upon complexation. Excitation wavelength at 430 nm. c = ~5 x 10^{-6} M.

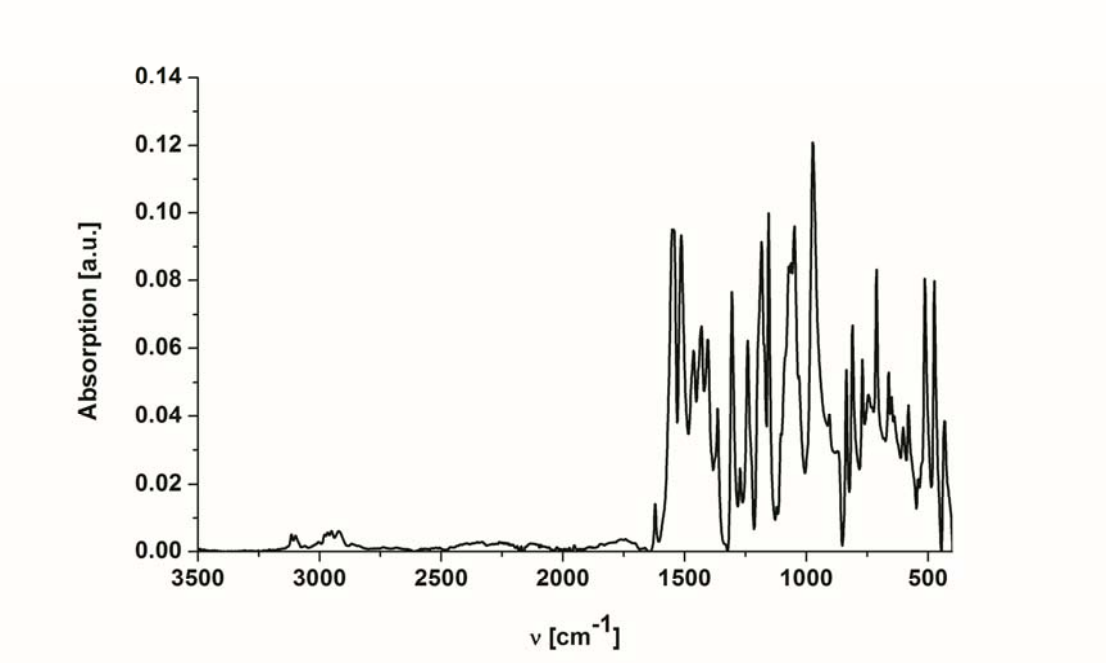

Figure S14. Solid state ATR-FT-IR spectrum of **1**.

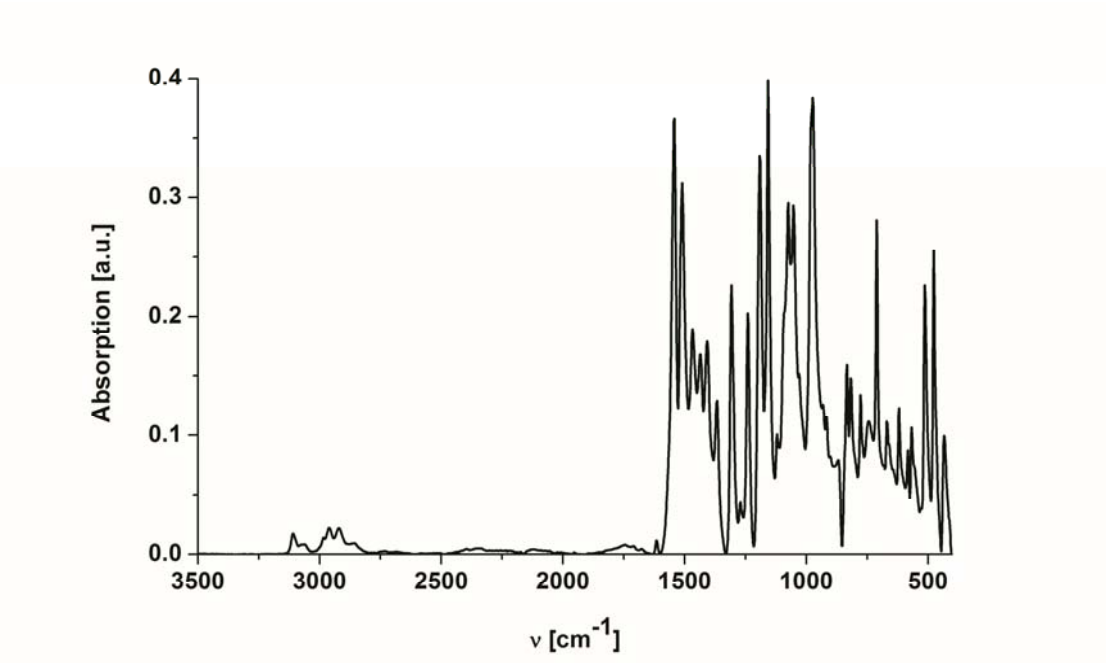

Figure S15. Solid state ATR-FT-IR spectrum of **2**.

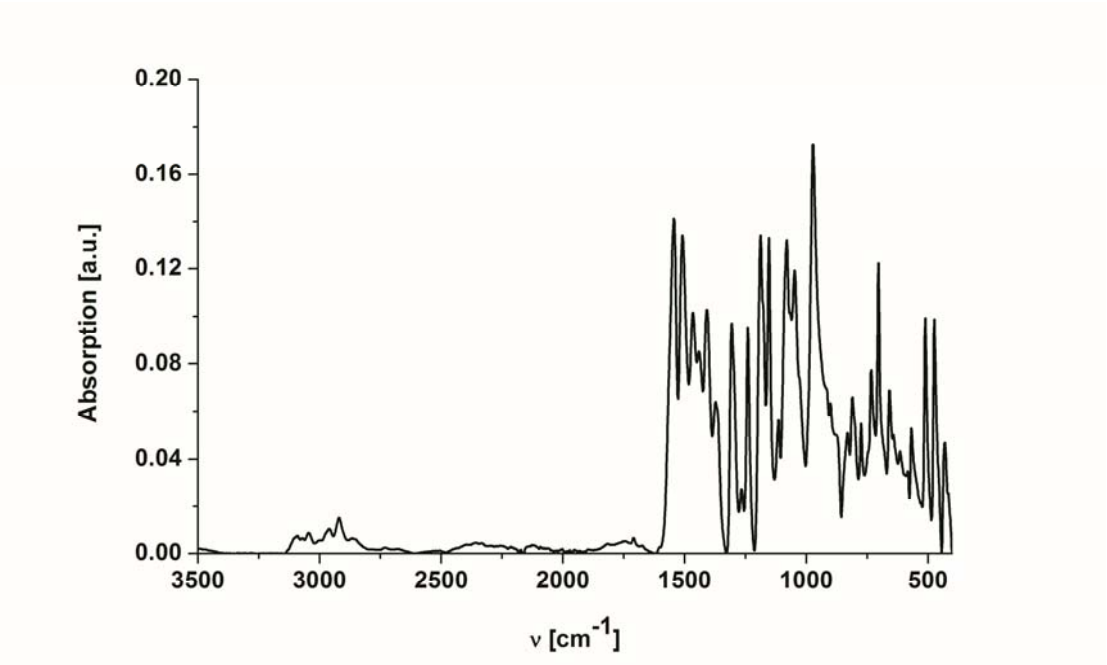

Figure S16. Solid state ATR-FT-IR spectrum of **3**.

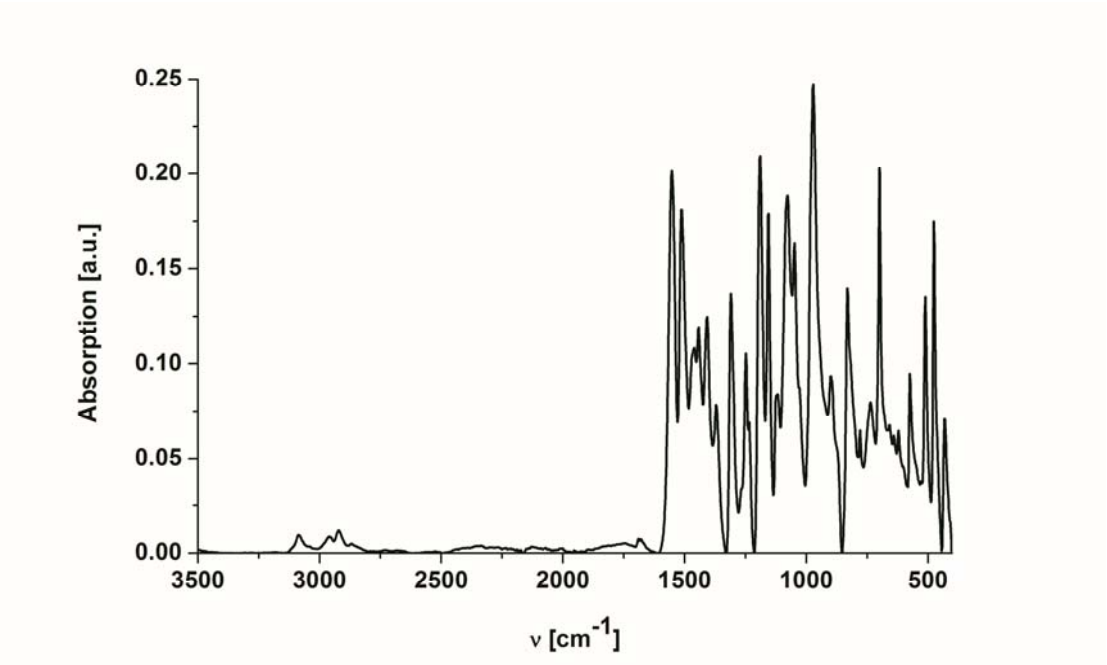

Figure S17. Solid state ATR-FT-IR spectrum of **4**.

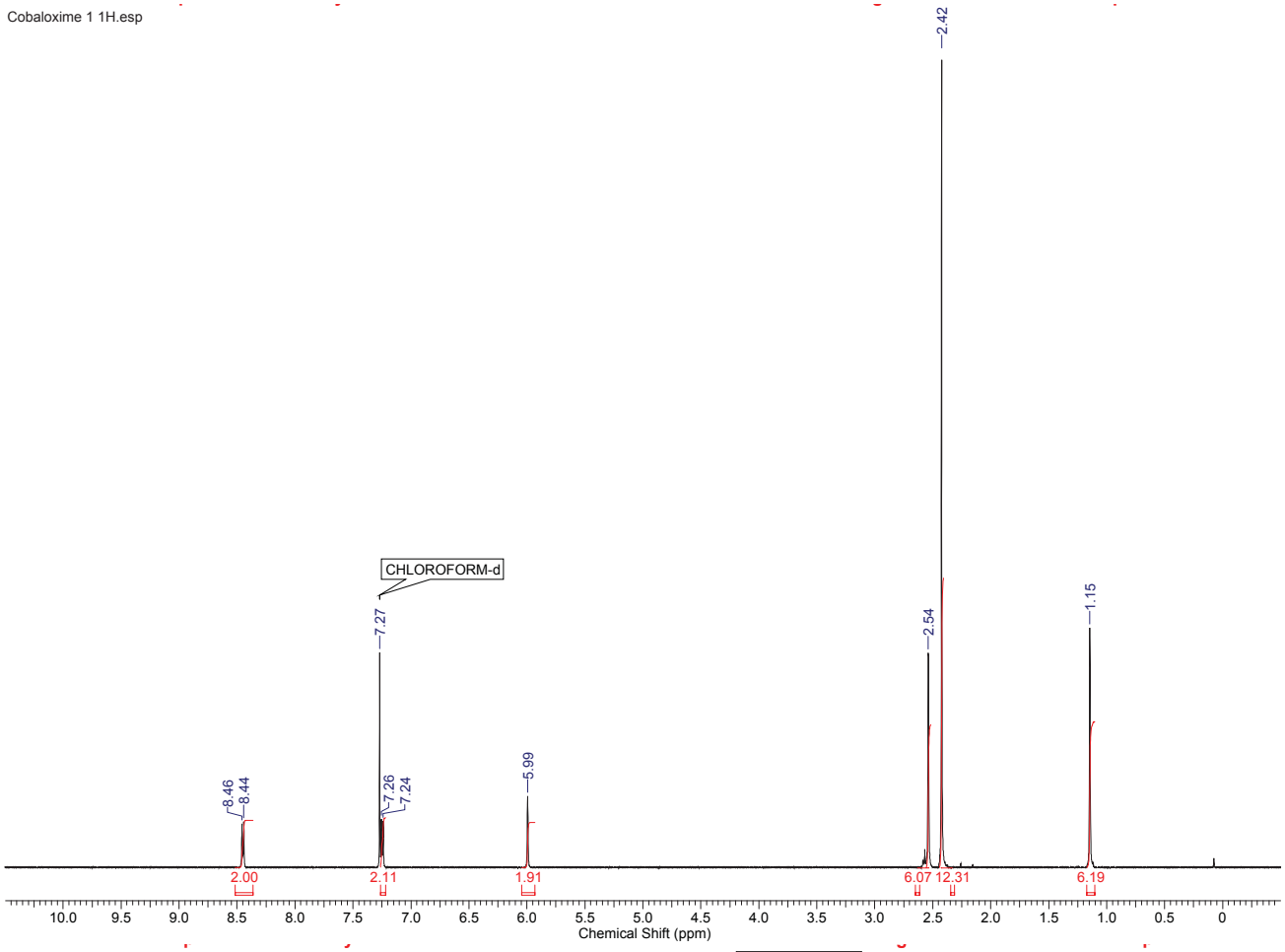
Cobaloxime 1 1H.esp
CHLOROFORM-d
2.42
7.27
2.54
1.15
8.46
8.44
7.26
7.24
5.99
2.00
2.11
1.91
6.07
12.31
6.19
Chemical Shift (ppm)

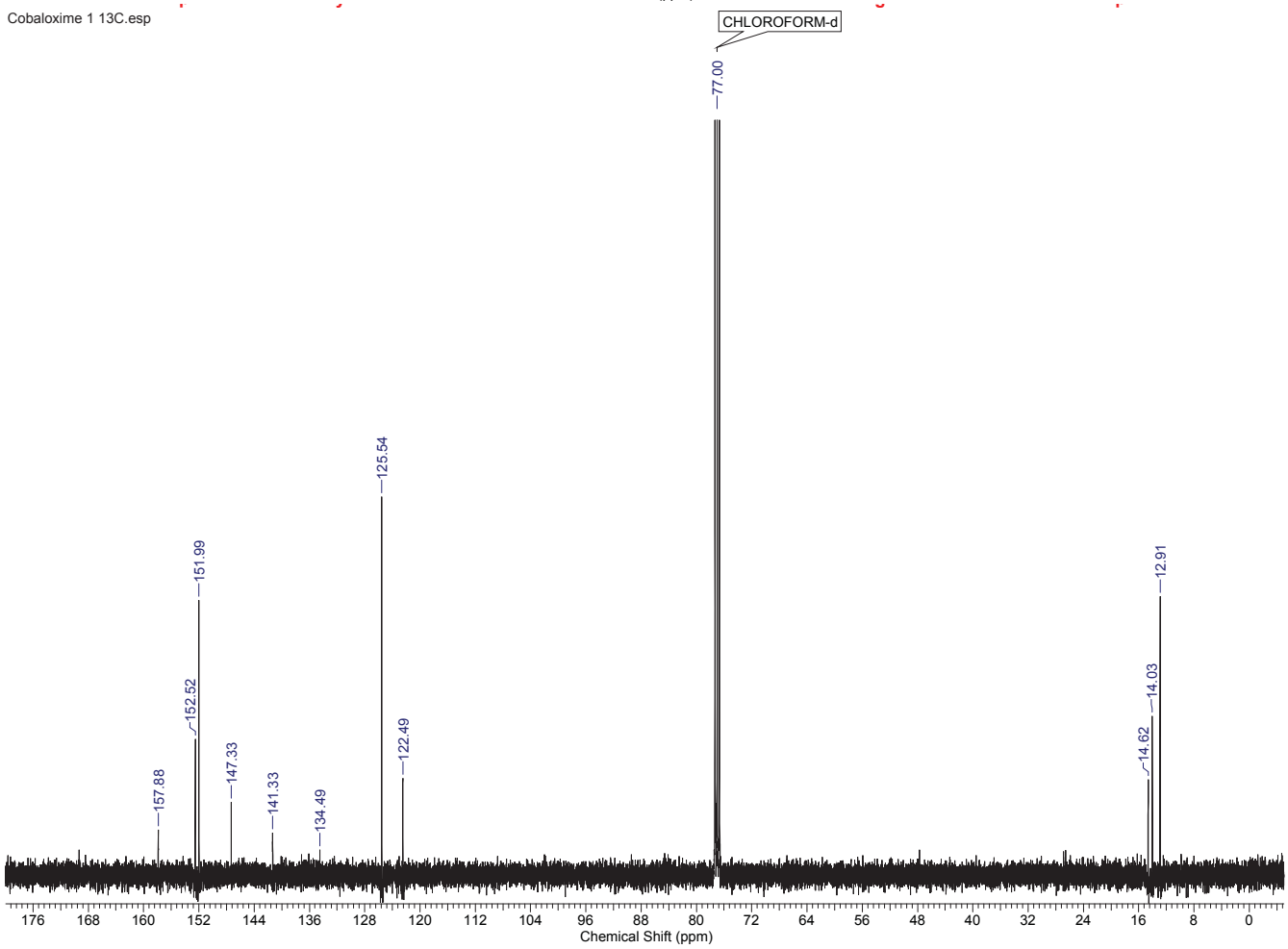
Cobaloxime 1 13C.esp
CHLOROFORM-d
77.00
125.54
151.99
152.52
157.88
147.33
141.33
134.49
122.49
12.91
14.03
14.62
Chemical Shift (ppm)

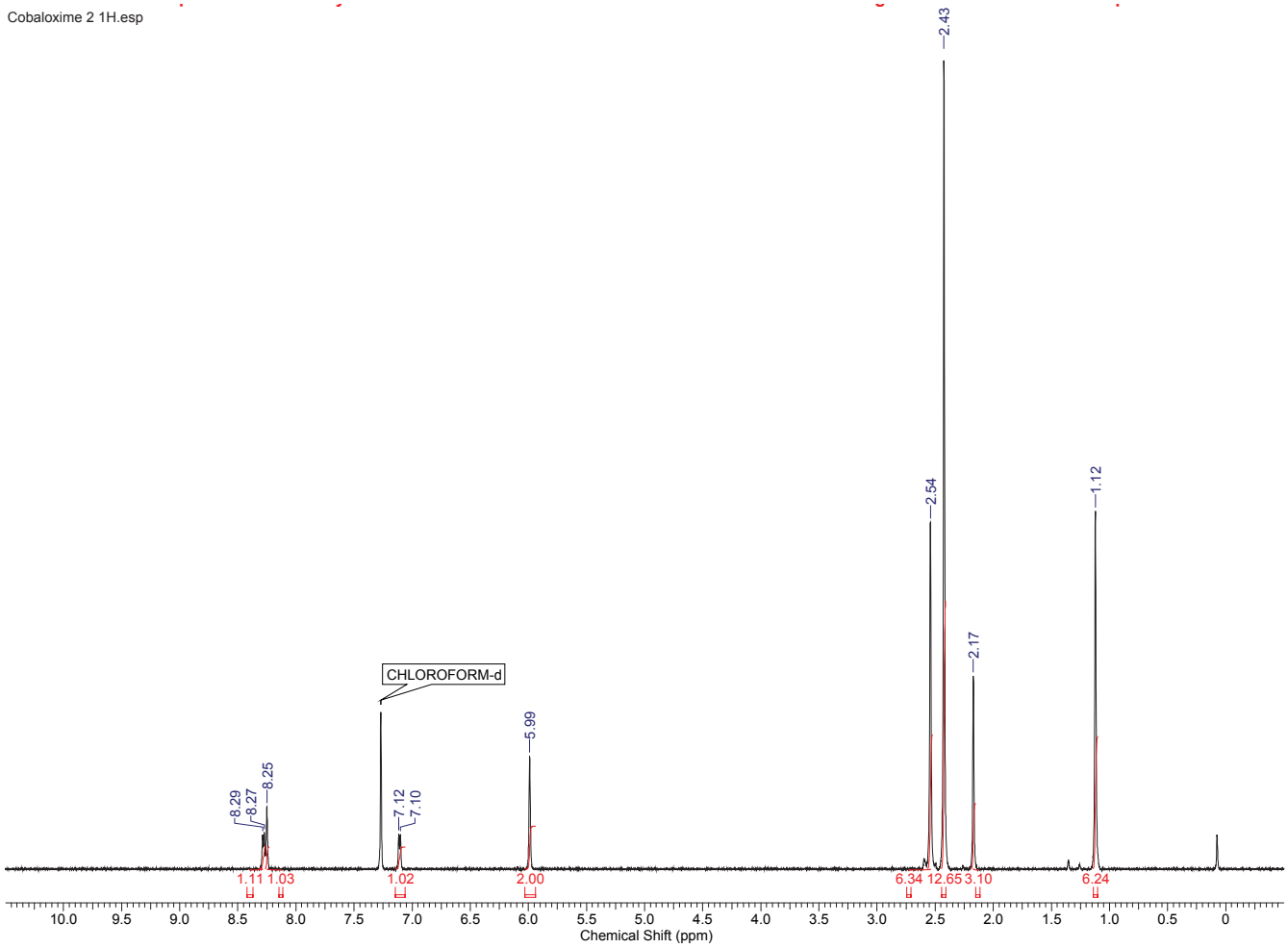
Cobaloxime 2 1H.esp
2.43
2.54
1.12
2.17
CHLOROFORM-d
5.99
8.29
8.27
8.25
7.12
7.10
1.11 1.03
1.02
2.00
6.34 12.65 3.10
6.24
Chemical Shift (ppm)

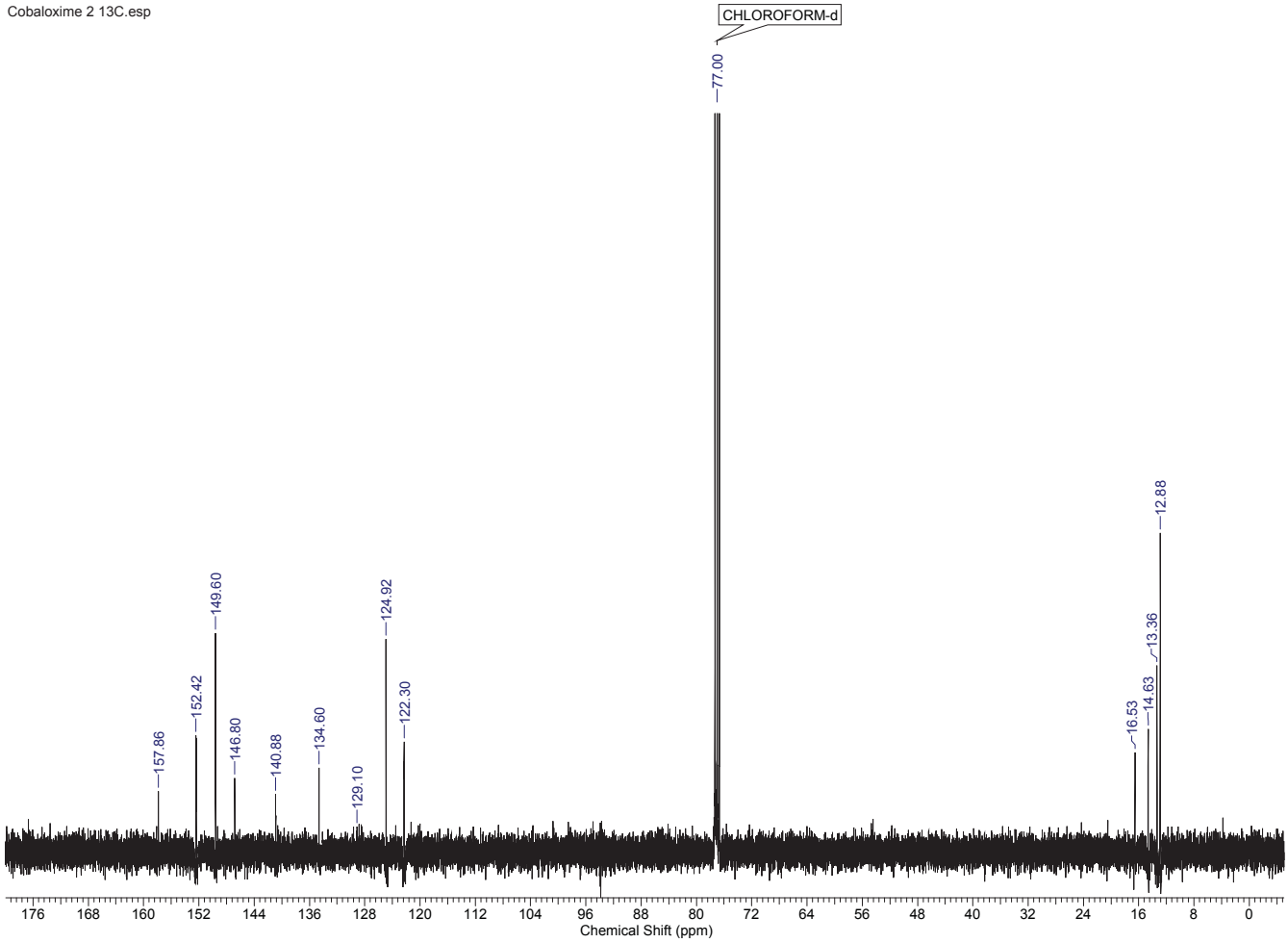
Cobaloxime 2 13C.esp
CHLOROFORM-d
77.00
157.86
152.42
149.60
146.80
140.88
134.60
129.10
124.92
122.30
16.53
14.63
13.36
12.88
Chemical Shift (ppm)

Cobaloxime 3 1H.esp

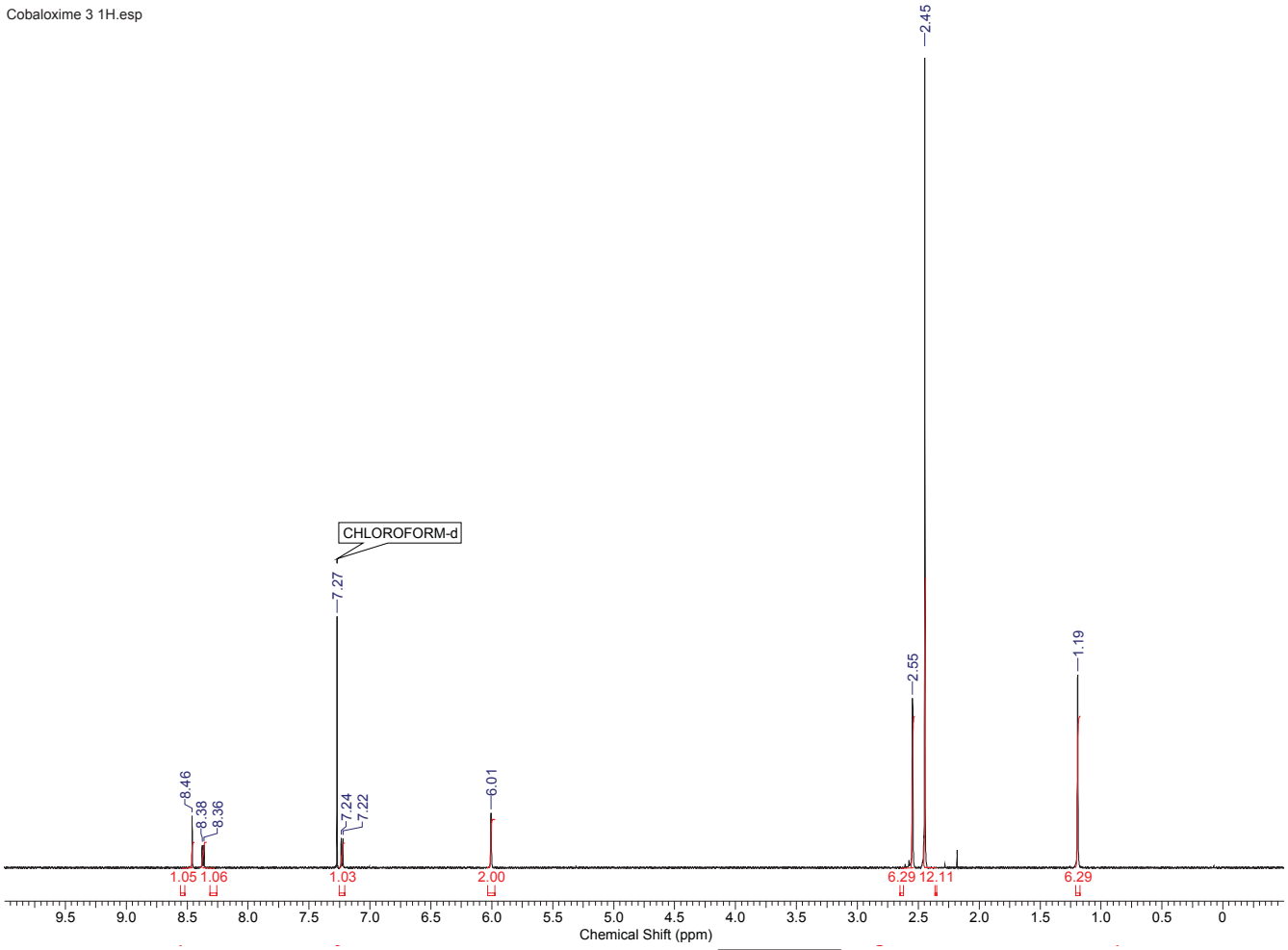

Cobaloxime 3 13C.esp

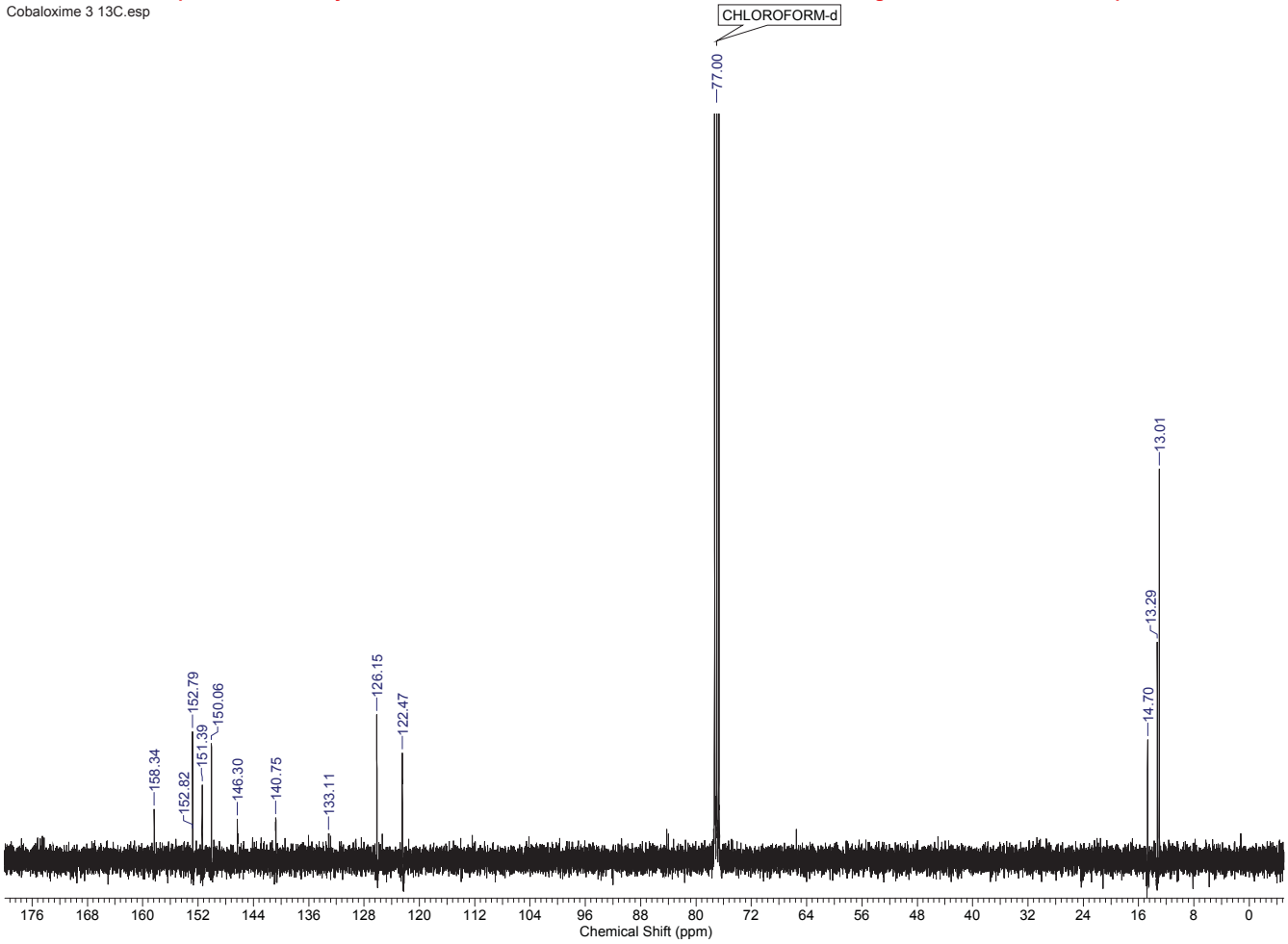

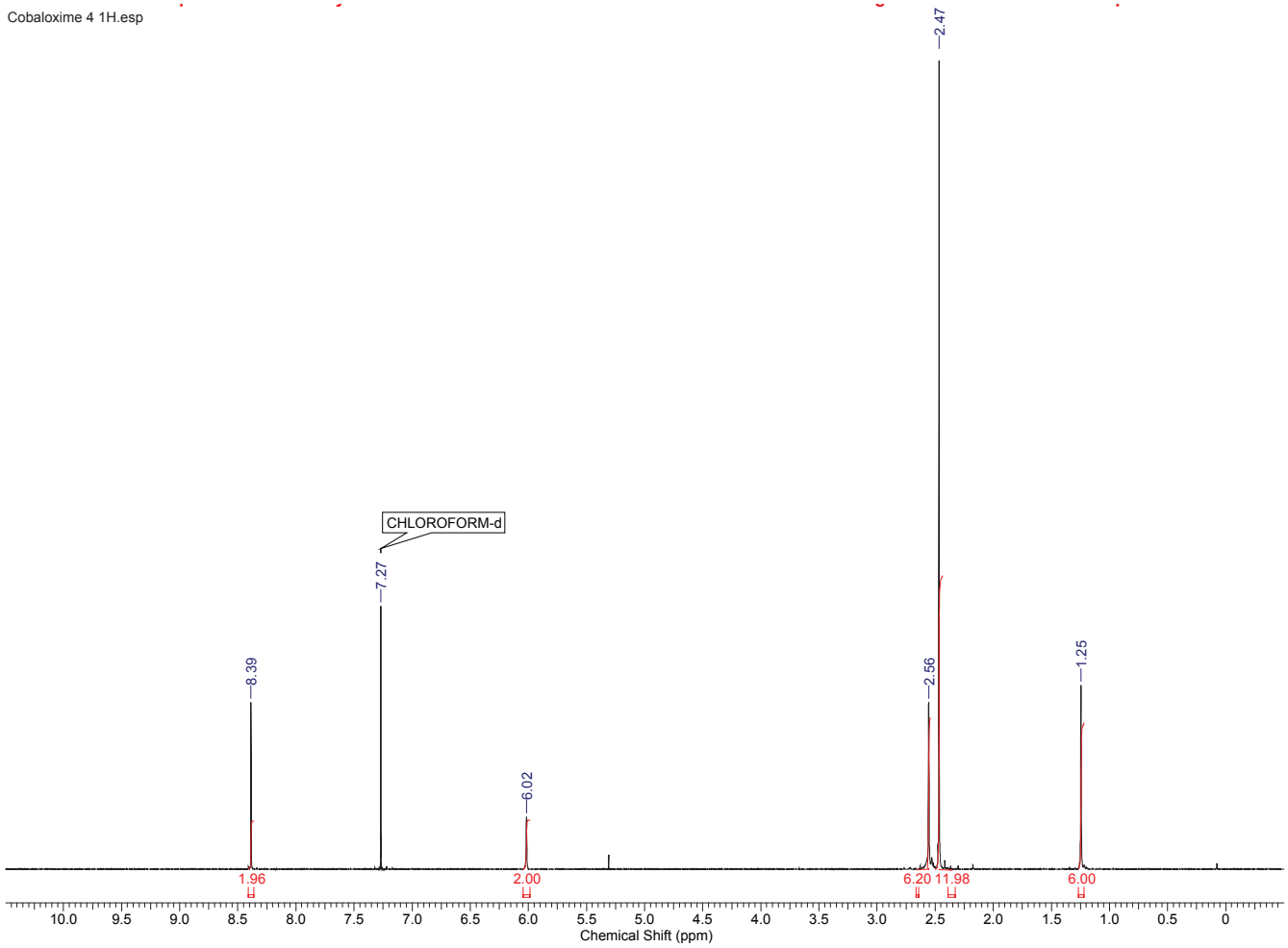
Cobaloxime 4 1H.esp
CHLOROFORM-d
2.47
7.27
8.39
6.02
2.56
1.25
1.96
2.00
6.20
11.98
6.00
Chemical Shift (ppm)

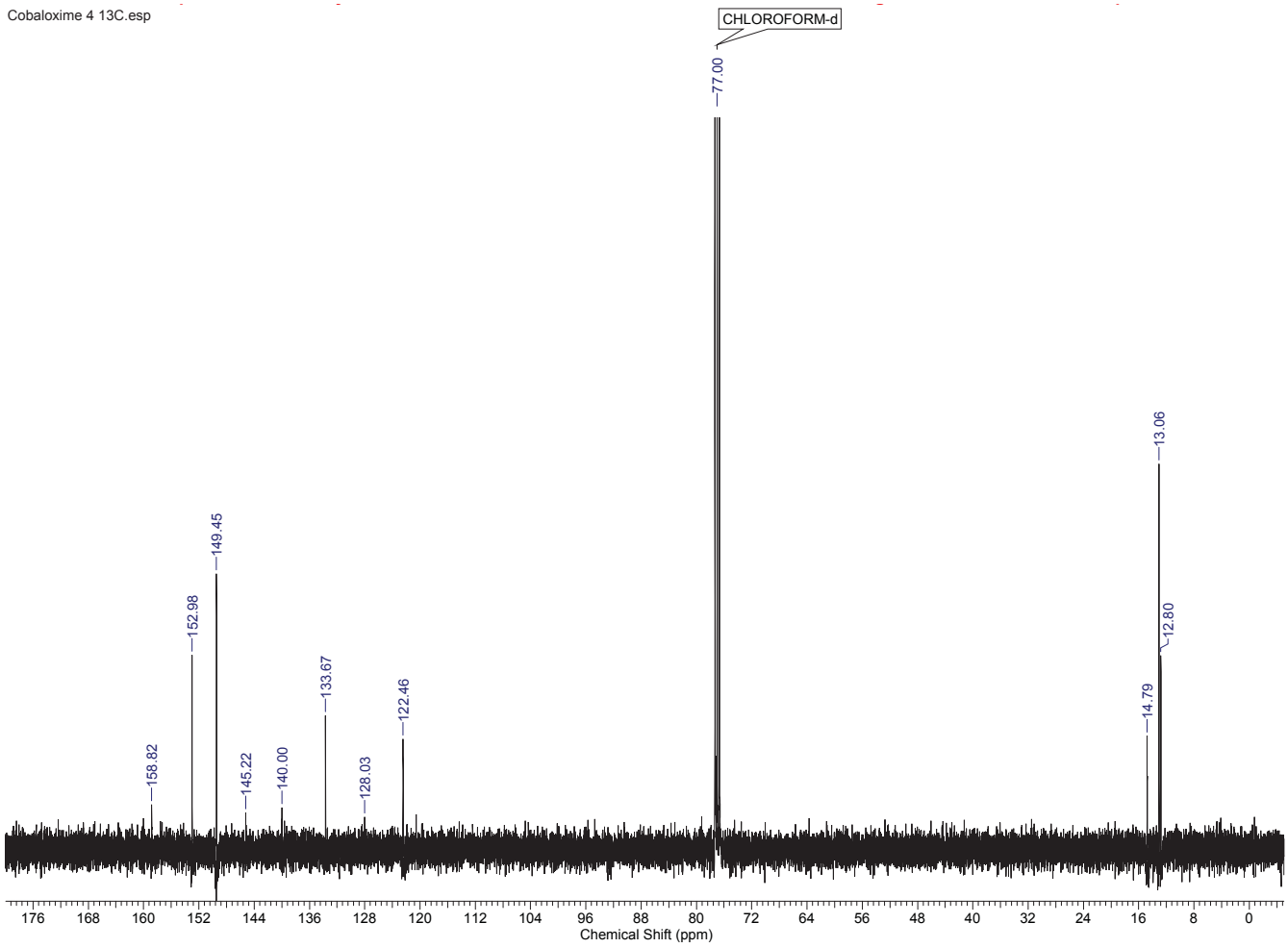
Cobaloxime 4 13C.esp
CHLOROFORM-d
77.00
13.06
12.80
14.79
149.45
152.98
133.67
122.46
158.82
145.22
140.00
128.03
Chemical Shift (ppm)